INTERNATIONAL JOURNAL FOR NUMERICAL METHODS IN FLUIDS, VOL. 15, 865–881 (1992)

NUMERICAL SIMULATION OF A LOW-EMISSION GAS TURBINE COMBUSTOR USING KIVA-II

S. L. YANG* AND R. CHEN†

ME-EM Department, Michigan Technological University, 1400 Townsend Drive, Houghton, MI 49931-1295, U.S.A.

M. C. CLINE

Los Alamos National Laboratory, Los Alamos, NM, U.S.A.

H. L. NGUYEN

NASA Lewis Research Center, Cleveland, OH, U.S.A.

AND

G. J. MICKLOW

University of Florida, Gainesville, FL, U.S.A.

SUMMARY

A numerical study was performed to investigate chemically reactive flows with sprays inside a staged turbine combustor (STC) using a modified version of the KIVA-II code. This STC consists of a fuel nozzle (FN), a rich-burn (RB) zone, a converging connecting pipe, a quick-quench (QQ) zone, a diverging connecting pipe and a lean-combustion (LC) zone. From the computational viewpoint, it is more efficient to split the STC into two subsystems, called FN/RB zone and QQ/LC zones, and the numerical solutions were obtained separately for each subsystem. This paper addresses the numerical results of the STC which is equipped with an advanced airblast fuel nozzle. The airblast nozzle has two fuel injection passages and four air flow passages. The input conditions used in this study were chosen similar to those encountered in advanced combustion systems. Preliminary results generated illustrate some of the major features of the flow and temperature fields inside the STC. Velocity, temperature and some critical species information inside the FN/RB zone are given. Formation of the co- and counter-rotating bulk flow and the sandwiched-ring-shaped temperature field, typical of the confined inclined jet-in-cross-flow, can be seen clearly in the QQ/LC zones. The calculations of the mass-weighted standard deviation and the pattern factor of temperature revealed that the mixing performance of the STC is very promising. The temperature of the fluid leaving the LC zone is very uniform. Prediction of the NO_x emission shows that there is no excessive thermal NO_x produced in the QQ/LC zones for the case studied. From the results obtained so far, it appears that the modified KIVA-II code can be used to guide the low-emission combustion experiments.

KEY WORDS Gas turbine combustors CFD Emissions Airblast atomizers Dilution jet mixing

* Assistant Professor, to whom correspondence should be addressed.
† Graduate Research Assistant.

0271–2091/92/200865–17$13.50

Received 25 November 1991
Revised 4 May 1992

INTRODUCTION

The current environmental issue on pollution imposes an urgent need in the reduction of NO_x emission from gas turbine engines. One way to reduce the production of NO_x from the gas turbine combustor is to utilize the staged turbine combustor (STC) concept.[1-4] One STC, which consists of a fuel nozzle (FN), a rich-burn (RB) zone, a converging connecting pipe, a quick-quench (QQ) zone, a diverging connecting pipe and a lean-combustion (LC) zone, is shown in Figure 1. The STC concept incorporates staged burning. Combustion is initiated in the RB zone with an equivalence ratio, ϕ, in the range 1·2–2·0. The hydrocarbon reactions proceed rapidly, depleting the available oxygen, thereby inhibiting NO_x formation. The hot rich mixture is then rapidly diluted and mixed by an array of air dilution holes or slots in the QQ zone. The combustion is completed with ϕ in the range 0·4–0·6 stoichiometric in the LC zone. The STC concept offers a broad operational range because of the good flame stability of the RB zone. It is also known that one key element for successful reduction of NO_x from the exhaust of STC is the proper design of dilution jet mixing in the QQ zone. Therefore, to increase the performance efficiency and to reduce the NO_x pollutant emissions, the mixing process becomes essential to the design of STC.

Numerical simulation of gas turbine combustors has become increasingly more important in the past decade. Solutions obtained by numerical methods are often used to assist experimental studies which, in turn, will save time and money by reducing the number of tests and possible hardware modifications. However, complete numerical studies of potential complex STC are still in their infancy. The most recent studies dealing with the QQ zone dilution jet mixing problems in flametube combustors can be found in References 5–9.* In their approach, the fluid and thermodynamic properties at the inlet of the QQ zone were assumed to be uniform and were estimated by a one-dimensional model for the RB zone. Their main focus was on the dilution jet mixing inside the QQ zone. Parameters such as the momentum flux ratio, slot aspect ratio and mixing flow area were investigated.

There are several approaches that can be used to numerically solve the chemically reactive fluid flow and heat transfer occurring inside the STC shown in Figure 1. One is to consider the whole

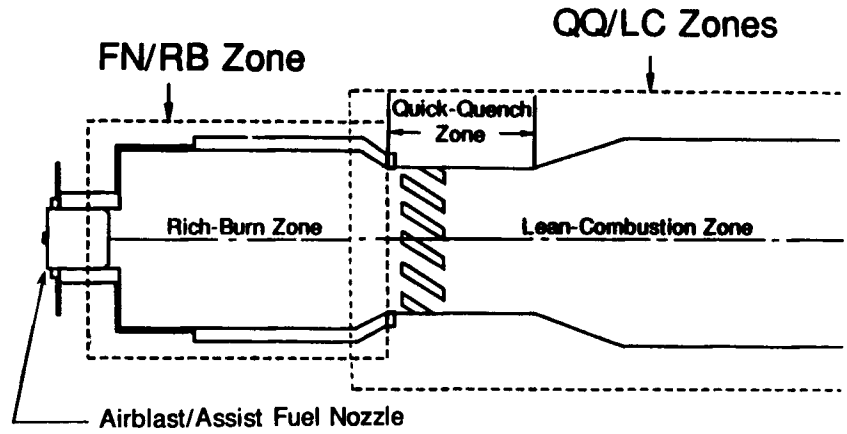

Figure 1. Schematic diagram of a staged turbine combustor

* Reference 8 included the RB zone (premixed, prevaporized) and, therefore, the swirl entering the QQ zone was not assumed.

combustor as a single unit. Another is to isolate each zone with the interrelations between zone treated through the inlet/outlet boundary conditions. For instance, the outlet condition of the RB zone can be used as the inlet condition of the QQ zone. This allows the zones to be treated differently. For example, the RB zone can be assumed to be axisymmetric (with swirl) while the QQ zone must be considered to be three-dimensional due to the discrete slots. Therefore, for computational efficiency, the RB zone was calculated as an axisymmetric problem with a finer mesh to resolve the airblast nozzle passages. The QQ zone was calculated as a three-dimensional problem using a coarser sector mesh to isolate one slot. In this paper, the STC was divided into two subsystems, called FN/RB zone and QQ/LC zones, and the numerical solutions were obtained separately for each subsystem with a considerable amount of zone overlap to minimize the effect of interzone boundary conditions.

The purpose of this paper is to present a multidimensional numerical solution of the turbulent two-phase reacting flows inside the STC using a modified version of the KIVA-II code.[10] The conditions at the FN/RB zone inlet and the slot opening (dilution jet) were chosen similar to those encountered in advanced combustion systems. Inlet conditions of the QQ/LC zones were not assumed but were obtained from the FN/RB zone results.

DESCRIPTION OF THE PROBLEM

To minimize the effect of the interzone boundary conditions, the outlet boundary of the FN/RB zone was extended to the end of the convergence section and the inlet boundary of the QQ/LC zones was extended 1·82 in upstream of the convergence section, which corresponds to one grid line in the FN/RB zone (see Figure 1 for the FN/RB zone and the QQ/LC zones computational sections). An advanced airblast nozzle was used as a means of supplying air and fuel for the RB zone. The airblast fuel nozzle has two fuel injection passages and four air flow passages. The inner flow passage has a counter-rotating swirler with a 63° van angle. The van angles of the middle, outer and dome flow passages are 61·3°, 60·2° and 60·2°, respectively, and are all co-rotating. In the QQ/LC zones, cool dilution air is injected into the QQ section through inclined slots. There were eight equally spaced 45° inclined slots located around the perimeter of the QQ zone. The centre of the slots was located at $D/3$ from the inlet of the QQ zone, where D is the diameter of the QQ zone. The slot aspect ratio (length to width) was 6. Due to geometric symmetry, only one slot was modelled, resulting in a 45° sector, and the slot was symmetrically located at the centre plane of the sector. The diameters of RB, QQ and LC zones were in the ratio of 1·2 : 1 : 1·4. Figure 2 shows the geometry and dimensions used to model the FN/RB and QQ/LC zones. In this figure, L_{rich} and L_{quick} are the lengths of the RB and QQ zones, respectively.

FN/RB zone boundary conditions

The following inlet conditions, which are similar to those encountered in advanced combustion systems, were used:

temperature = 1000°F (811·1 K),
pressure = 90 psia ($6{\cdot}2 \times 10^6$ dyn/cm^2),
air mass flow rate = 1·1 lbm/s (494·4 g/s),
air flow split = 7·8/19·1/25·5/47·6% (from inner to dome),
air flow passage area = 0·007/0·0117/0·0156/0·027 ft^2 (6·50/10·87/14·49/25·08 cm^2),
equivalence ratio = 2·0,
fuel split = 50/50%,

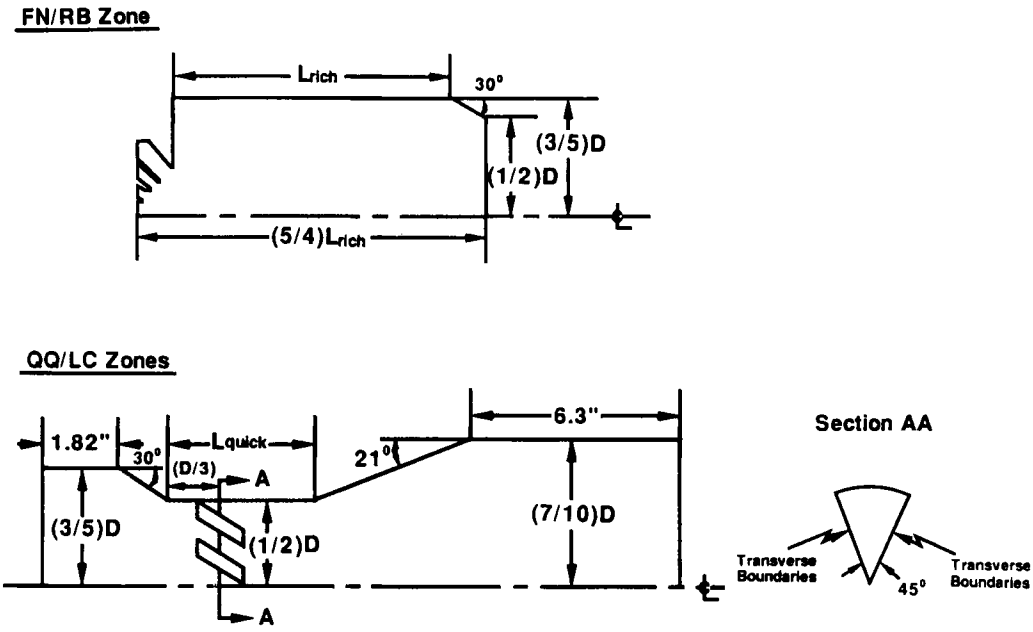

Figure 2. FN/RB and QQ/LC zones computational sections (The four air passage fuel nozzle is shown at the left end of the FN/RB zone. The lower and upper passages are the inner and dome air passages, respectively.)

turbulent length scale = 0·25 of the respective flow passage width,
turbulent kinetic energy = 1% of the respective $0{\cdot}5W^2$,

where W is the mean axial velocity at the inlet.

The inlet boundary conditions were the specification of the density (calculated from the temperature and pressure given above) and W (calculated from the mass flow rates and flow areas given above). The radial velocity component was set so that the inlet flow was tangential to the flow passages. The azimuthal or swirl velocity component was specified, assuming wheel flow. The turbulent kinetic energy and length scale were specified at the values given above. The exit boundary condition was to specify the pressure. The combustor walls were assumed to be adiabatic with a turbulent boundary layer. These conditions were enforced using wall functions.[10]

QQ/LC zones boundary conditions

At the mainstream inflow boundary, the hot rich mixture from the FN/RB zone enters the QQ/LC section. A tension spline interpolation[11,12] was then used to interpolate the necessary information at the inlet. The actual boundary conditions were the specification of the three velocity components, density, turbulent kinetic energy and the turbulent length scale. Because the flow is subsonic, the pressure and temperature cannot be specified, but instead must be calculated as part of the solution. If the calculated pressure does not differ significantly from the RB zone value at the same location then the solution is assumed to be complete. However, if the calculated pressure differs significantly then the RB zone solution must be repeated. The new outflow boundary condition for the RB zone would be the pressure obtained from the QQ zone solution. This process would be repeated as necessary.

At the jet inflow boundary, the dilution jet was air (consisting of 76·8% N_2 and 23·2% of O_2) and entered the inclined slot with uniform radial velocity. The following jet inlet conditions were

chosen:

temperature = 1000°F (811·1 K),
pressure = 90 psia ($6{\cdot}2 \times 10^6$ dyn/cm^2),
jet-to-mainstream momentum flux ratio ($J = \rho_j V_j^2 / \rho_\infty V_\infty^2$) = 60,
turbulent length scale = 0·13 of D,
turbulent intensity = 0·1 of V_j,

where V_j and ρ_j are the jet inflow radial mean speed and density, respectively, and the subscript ∞ refers to the mainstream flow condition. The slot flow area was modified to maintain a constant jet-to-mainstream mass flow rate ratio (MJMR) of 3 and a slot orifice discharge coefficient of 0·6. The jet inlet boundary conditions were the specification of ρ_j (calculated from the temperature and pressure given above) and V_j (calculated from J and MJMR given above). The turbulent intensity (v') and length scale were specified at the values given above, according to Talpallikar *et al.*[5,6] The exit boundary condition was to specify the pressure. The combustor walls were assumed to be adiabatic with a turbulent boundary layer. At the transverse boundaries (see Figure 2), periodic boundary conditions were applied.

NUMERICAL METHOD OF SOLUTION

The problem was modelled as a compressible turbulent reacting flow and was closed by a κ–ε turbulent model with wall function. The numerical solutions were obtained by a modified version of KIVA-II, implemented to study the aforementioned objective.

The KIVA-II code

The KIVA-II code,[10] developed at the Los Alamos National Laboratory, is an advanced computer program for the numerical calculation of transient, two- and three-dimensional, chemically reactive fluid flows with sprays. It solves the unsteady equations of motion of a turbulent, chemically reactive mixture of ideal gases, coupled to the equations for a single-component vapourizing fuel spray. The numerical scheme is based on the arbitrary Lagrangian–Eulerian (ALE) method[13,14] with implicit continuous Eulerian modification for low Mach number flows. A stochastic particle method is used to calculate the evaporation rate of liquid sprays. The effects of droplet oscillation, distortion, breakup, collision and coalescence are considered in the computations. Several upwind convection schemes, such as the partial donor cell and quasi-second-order upwind, are included. Two turbulence models, modified κ–ε and subgrid scale models, are also available. For additional details of the KIVA-II, see Reference 10.

Grid system

The FN/RB zone grid system (81×51 grid points) was generated by an algebraic/elliptic method and is given in Figure 3. In order to generate a grid system for the QQ/LC zones with inclined slots shown in Figure 4, an algebraic grid generation scheme[15] based on the transfinite interpolation method[16,17] was used. There are 21 points in the r direction, 19 points in the θ direction, and 51 points in the z direction. Note that, in Figure 4, a twisted mesh was used to obtain the inclined-slot configuration. The details of how this mesh was generated can be found in Reference 15.

To see the effect of this twisted mesh on the solutions, a pure pipe flow with uniform inlet and without swirl was run for the grid system with and without twisting. It was found that the fictitious swirl due to the twisted mesh was less than 1% and was considered insignificant.

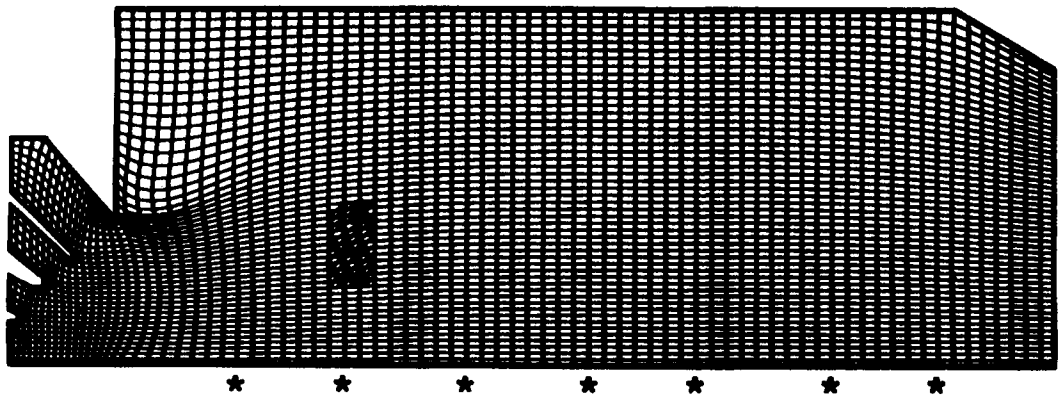

Figure 3. FN/RB zone computational mesh

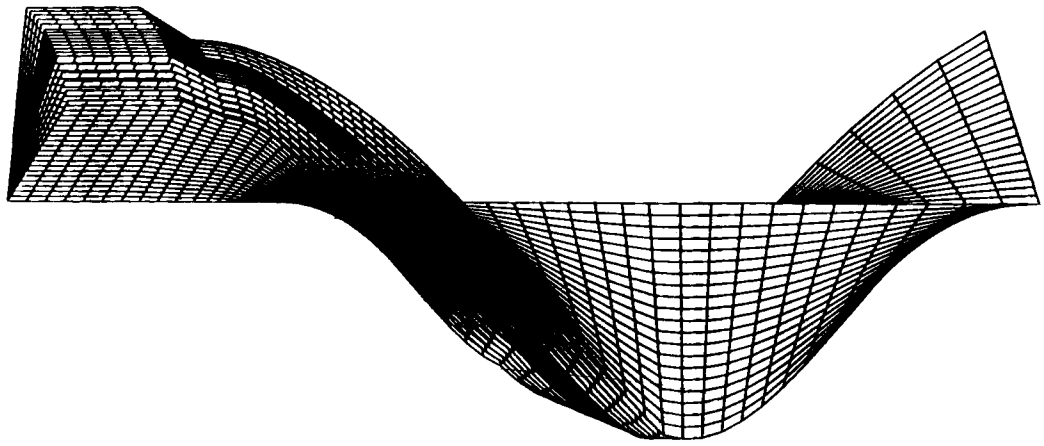

Figure 4. QQ/LC zones computational mesh

Code modifications

Since the KIVA-II is primarily written for solving the reciprocating internal combustion engine problems, modifications are needed for the application to the current problem. Following are the descriptions of the major changes made to the code.

The fuel was considered as jet-A in the liquid phase and propane in the gas phase, according to Nguyen and Ying.[18] The propane combustion was modelled using a simplified 11-reaction set (five kinetic reactions and six equilibrium reactions). The five kinetic reactions are:

$$C_3H_8 + (3/2 + 8/4)O_2 \leftrightarrow 3CO + 4H_2O,$$

$$CO + (1/2)O_2 \leftrightarrow CO_2,$$

$$O + N_2 \leftrightarrow N + NO,$$

$$O_2 + N \leftrightarrow O + NO,$$

$$N + OH \leftrightarrow H + NO,$$

and the six equilibrium reactions are:[19]

$$H_2 \leftrightarrow 2H,$$
$$O_2 \leftrightarrow 2O,$$
$$N_2 \leftrightarrow 2N,$$
$$O_2 + H_2 \leftrightarrow 2OH,$$
$$O_2 + 2H_2O \leftrightarrow 4OH,$$
$$O_2 + 2CO \leftrightarrow 2CO_2.$$

The details of this simplified chemical reaction model together with the reaction constants can be found in Reference 18.

FN/RB zone modifications

The grid system, given above, was generated separately, and the KIVA-II code was modified to read the grid information accordingly in the input data routine. The geometry routines were modified to allow four separate inlet flow passages to be defined. The boundary condition routines were modified to allow separate inlet conditions for each passage. In addition, the boundary condition routines were modified to allow arbitrary-shaped combustor walls. Properties of jet-A liquid fuel were also added to the code.

Species information both at the inflow and fuel sprays were specified and the necessary modifications were made to include the number of species and their thermodynamic properties. Calculations of the emission index of CO and NO were also included. The emission index was defined as the ratio of the grams of pollutant formed divided by the kilograms of fuel consumed.

QQ/LC zones modifications

In addition to the modifications made to the basic KIVA-II code described above, further modifications are needed for the study of the QQ/LC zones. Following are the descriptions of the additional changes made to the code.

The geometry routines were modified so that the dilution slot on the right wall (from KIVA-II view) can be identified. The boundary condition routines were modified such that the inflow information at the slot can be specified. The data input routine was also modified to read the inlet boundary information obtained from the FN/RB zone. Species information of air at the slot was also included.

To see the mixing effectiveness, the mass-weighted standard deviation (MWSD) and the pattern factor (PF) of temperature were selected and were included in the KIVA-II calculations. The MWSD and PF were defined as

$$\mathrm{MWSD} = \frac{\sqrt{\left[\sum_i m_i (T_i - T_{\mathrm{avg}})^2 \Big/ \sum_i m_i\right]}}{T_{\mathrm{avg}}}, \tag{1}$$

$$\mathrm{PF} = \frac{T_{\max} - T_{\mathrm{avg}}}{T_{\mathrm{avg}} - T_{\mathrm{jet}}} \tag{2}$$

according to Reference 5. The lower the values of MWSD and PF, the better is the mixing that can be achieved.

RESULTS AND DISCUSSION

Preliminary results were obtained using the quasi-second-order upwind scheme in the KIVA-II code. In the calculation of spray droplets, only the evaporation submodel was used.

FN/RB zone results

To closely simulate a real engine operating procedure, the code was executed as follows. At the beginning, the fuel sprays and ignition were turned off and the program was run with air only for 1000 time steps, which corresponds to 18·871 ms real-time simulation. Shortly after the cold run, both fuel injectors and ignitor were turned on at 18·872 ms. The ignitor was turned on for 1 ms and the location of the ignition window is shown in the crosshatched area in Figure 3. The reciprocal time constant for ignition energy addition to the ignition cells was set to $2{\cdot}61 \times 10^3$ in the KIVA-II input data file.

Figure 5 shows the steady-state velocity and temperature fields and the distribution of the liquid fuel particles. There are two recirculation zones, one located near the centre line and the

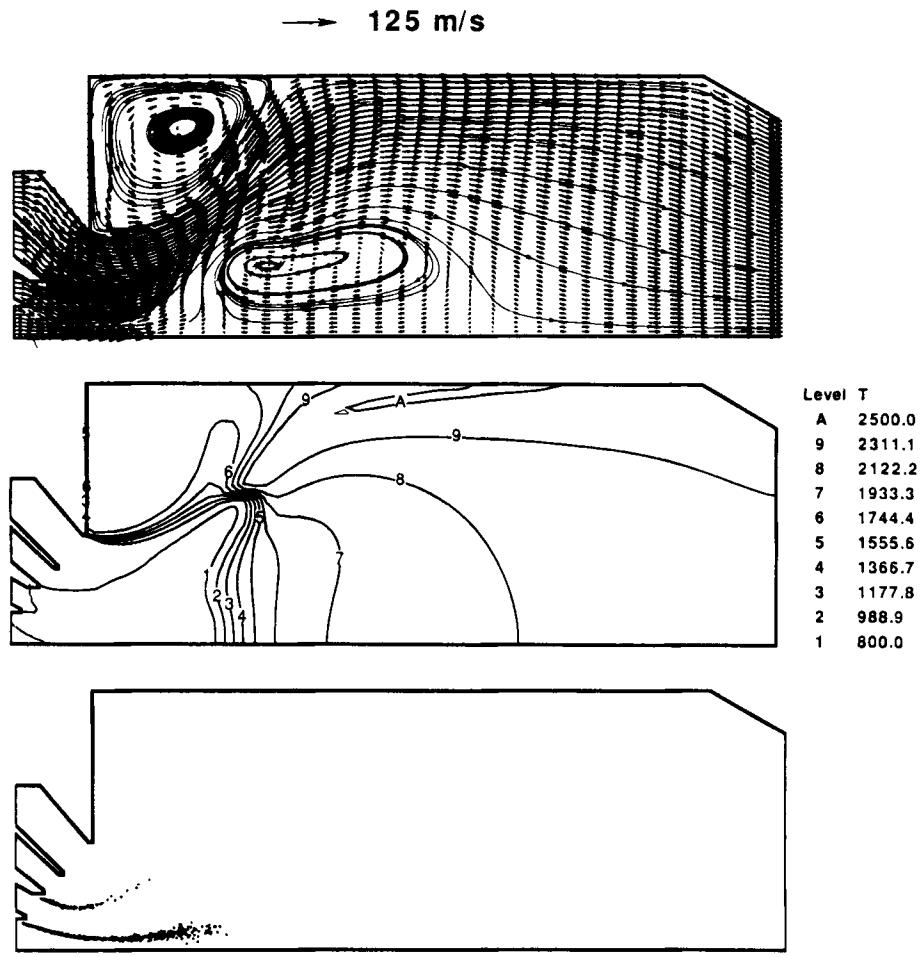

Figure 5. FN/RB zone velocity and temperature fields and the distribution of the liquid fuel particles

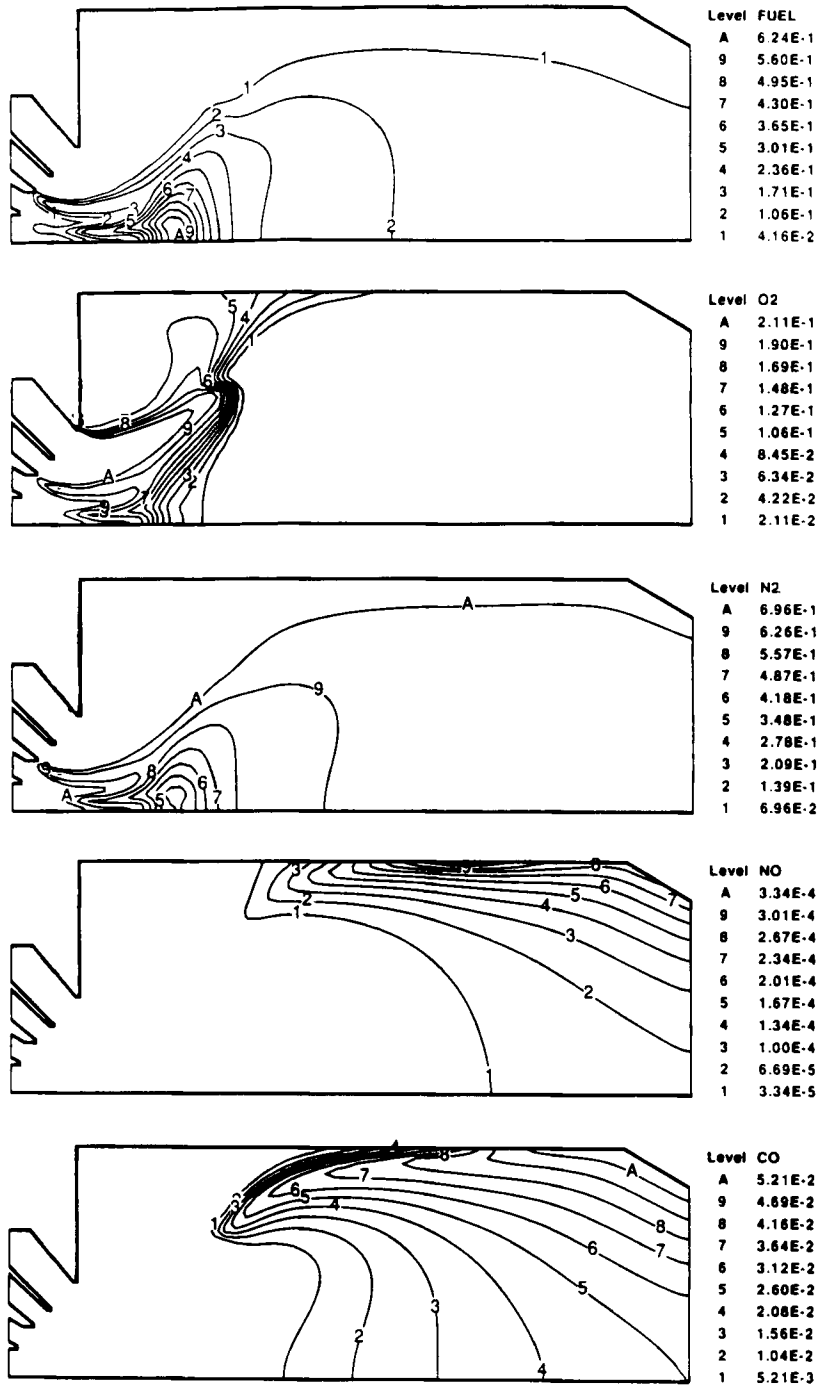

Figure 6. FN/RB zone species mass fraction contours

other at the left upper corner (typical to the combustor geometry under study), which can be seen clearly. The size and shape of the centre-line recirculation zone has an important influence on the performance of the RB zone. A parametric study of this aspect is currently under study. From the isotherm plot, it is seen that there is a high-temperature gradient region right after the isotherm level 1. The higher-temperature mixture is convecting downstream except the level A contour, which corresponds to the highest temperature shown in this figure under the current operating conditions. This local high-temperature region will create some impacts on NO formation (to be discussed next) and the design of the combustor liner thermal protection.

To have a better understanding of the temperature and velocity fields just described, contour plots of the mass fraction of fuel (in gas phase), O_2, N_2, NO and CO are given in Figure 6. From these contour plots, several observations can be made: (1) Due to the fuel-rich mixture ($\phi = 2{\cdot}0$) initiated at the fuel nozzle, the fuel contour plot shows that a certain amount of the unburned fuel still remains in the RB zone before entering the QQ section: (2) From the O_2 contour plot, one can see clearly that the available O_2 has been totally consumed at the very early stage of the chemical reactions: (3) A comparison of the isotherms and the O_2 contour plots near the crowded contour lines shows the similarity of these contours, indicating the location of the flame: (4) From the fuel and the N_2 contour plots and the cross reference with the flow field, it is seen that both fuel and air are diffused into the flame and are following the flow field outside the centre-line recirculation zone: (5) A comparison of the isotherms and the NO contour plots indicates that higher levels of NO are formed in the higher-temperature regions and the highest level (level A) is located right next to the combustor wall in the highest-temperature region as described in the previous paragraph: (6) Formation of CO occurs right after the flame as shown in the CO contour plot. A careful examination of these observations is currently under study so that a better FN/RB zone design can be reached. The emission index of CO and NO, calculated at different axial locations indicated by stars in Figure 3, is given in Figure 7.

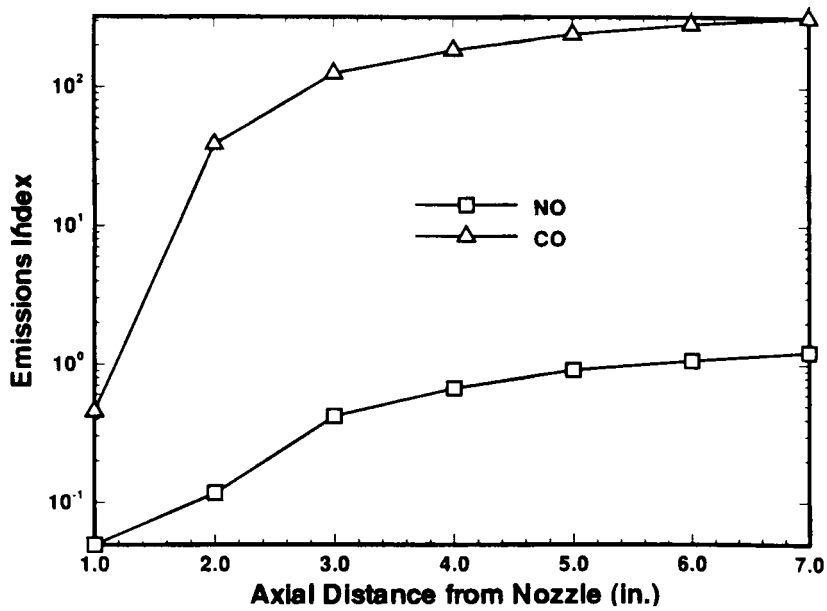

Figure 7. FN/RB zone CO and NO emission index

For the purpose of comparison, Figure 8 gives the flow field under pure flow condition (i.e. without fuel spray and chemical reaction). As one can see, without chemical reaction, the centre-line recirculation zone is very large. The results obtained from this part will be used as the inlet condition for the QQ/LC zones.

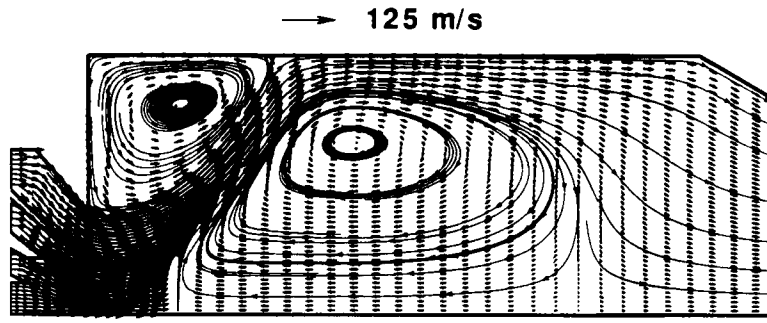

Figure 8. FN/RB zone pure flow velocity vectors

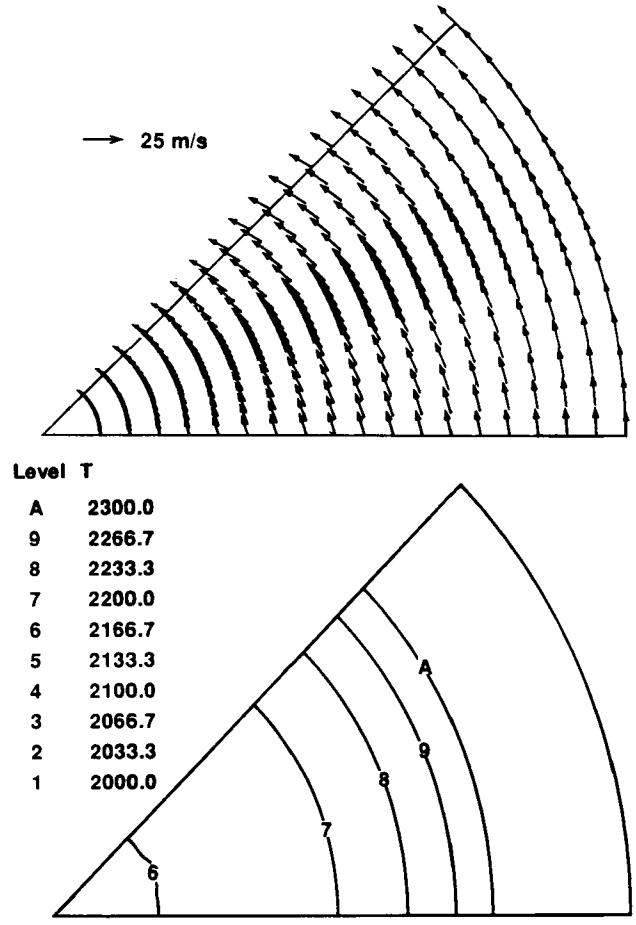

Figure 9. QQ/LC zones velocity vectors and isotherms at the inlet plane

QQ/LC zones results

Due to the twisted mesh, only the r–θ plane plots are given. Figure 9 shows the isotherms and the velocity vectors at the inlet, which were taken from the RB zone solutions at the location described in the 'Description of the problem' section. As one can see, the inlet conditions were non-uniform and with swirl. Accordingly, as done in the previous studies,[5–9] assuming uniform, non-swirling inlet conditions to the QQ zone would not be very accurate.

The velocity vectors and isotherms at the end of the slot opening are given in Figure 10. Due to the slanted slot, the two vortices, located on both sides of the jet, and the isotherms are not

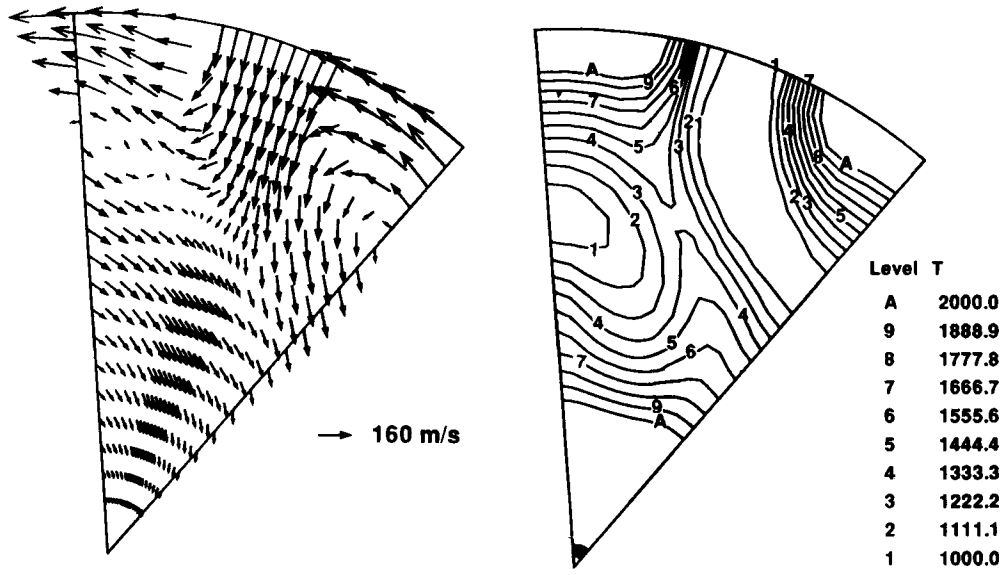

Figure 10. QQ/LC zones velocity vectors and isotherms at the end of the slot opening

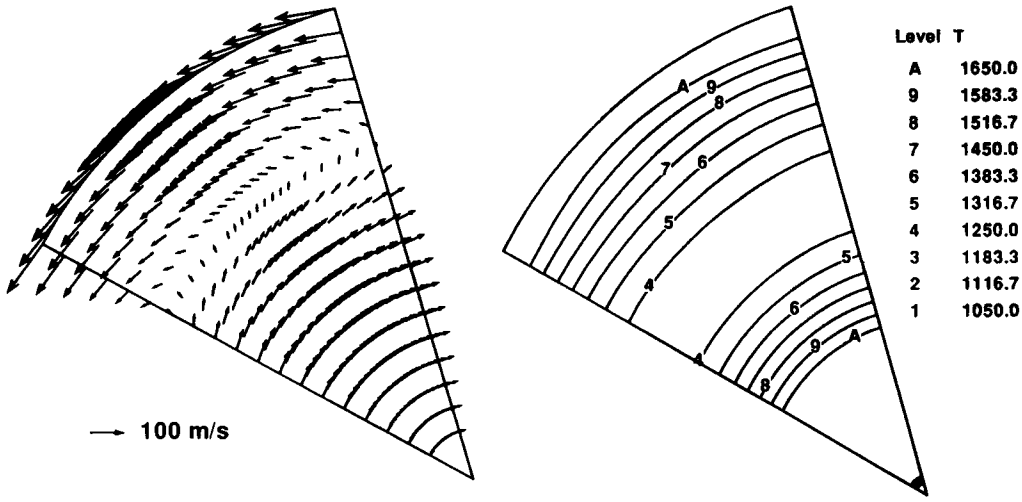

Figure 11. QQ/LC zones velocity vectors and isotherms at the beginning of the divergence section

symmetrical about the jet. It can be seen that, near the wall, the high-velocity dilution jet deflects the mainstream causing swirl, rotating in the direction parallel to the slot. However, near the axis, the mainstream deflects the dilution jet, setting up a counter-rotating swirl (in the main flow direction).

The interaction of the inclined jet with the mainstream fluid described above is the cause of the co- and counter-rotatng bulk flow pattern shown in Figure 11, in which the isotherms are also given. This is the plane located at the beginning of the divergence section. From Figure 11, there is a high-shear layer (HSL) separating the co- and counter-rotating bulk flows. From the isotherm plot, it can be seen that the HSL mainly contains the lower-temperature fluid, an indication of the effect of the jet penetration. The sandwiched-ring-shaped (for a whole circle) temperature field, in the order of hot–cold–hot, can be seen clearly in Figure 11. This bulk swirl flow and the

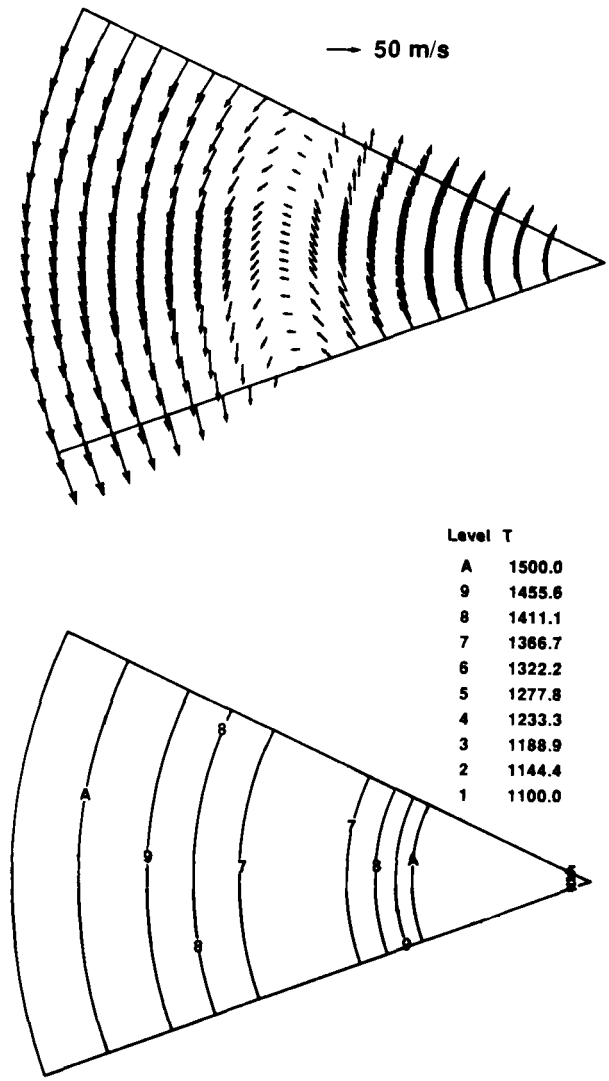

Figure 12. QQ/LC zones velocity vectors and isotherms at the end of the divergence section

sandwiched-ring-shaped isotherms, typical of the confined slanted jet-in-cross-flow, had been observed experimentally.[8]

The bulk swirl flow persists further downstream, as shown in Figure 12 (end of the divergence section). The HSL is moving toward the axis, which may be caused by the increasing flow cross-sectional area. At the exit of the LC zone, the bulk swirl flow has almost disappeared, as shown in Figure 13.

The values of MWSD and PF at various z locations are given in Figure 14. The peak shown in the figure is caused by the jet. It is observed from this figure that the fluid is well-mixed before leaving the LC zone, indicating that the mixing performance of the STC is very promising. Figure 15 gives the emission index of CO and NO at different z locations. Note that, in this figure, the x-axis represents the distance (in inches) downstream of the fuel nozzle. Prediction of the NO_x emission shows that there is no excessive thermal NO_x produced in the QQ/LC zones for the case studied.

The calculated mass-weighted average pressure at the inlet of the QQ/LC zones was 89·4 psia ($6{\cdot}164 \times 10^6$ dyn/cm^2) and the calculated value at the same location in the FN/RB zone was 89·3 psia ($6{\cdot}157 \times 10^6$ dyn/cm^2). Because this difference was very small, the calculations were not repeated to match the pressures.

CONCLUSIONS

In this study, numerical solutions of the chemically reactive flow inside the STC with an advanced airblast nozzle were obtained through a modified version of the KIVA-II code. In the QQ zone, cool dilution air was injected into the hot rich mixture through 45° inclined slots. The results obtained from the FN/RB zone were used as the inlet conditions for the QQ/LC zones. A tension spline interpolation scheme was then used to interpolate the necessary information needed. The

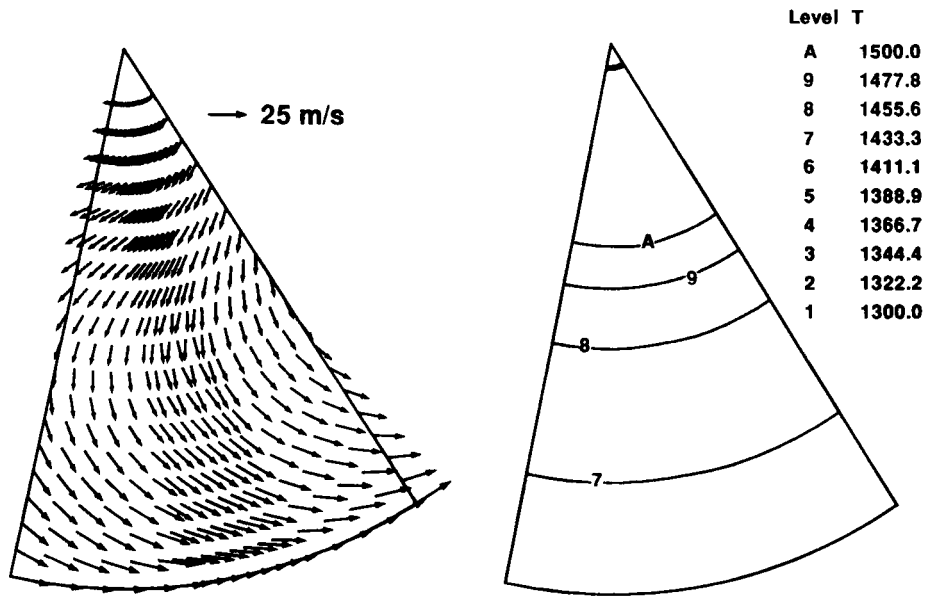

Figure 13. QQ/LC zones velocity vectors and isotherms at the outlet plane

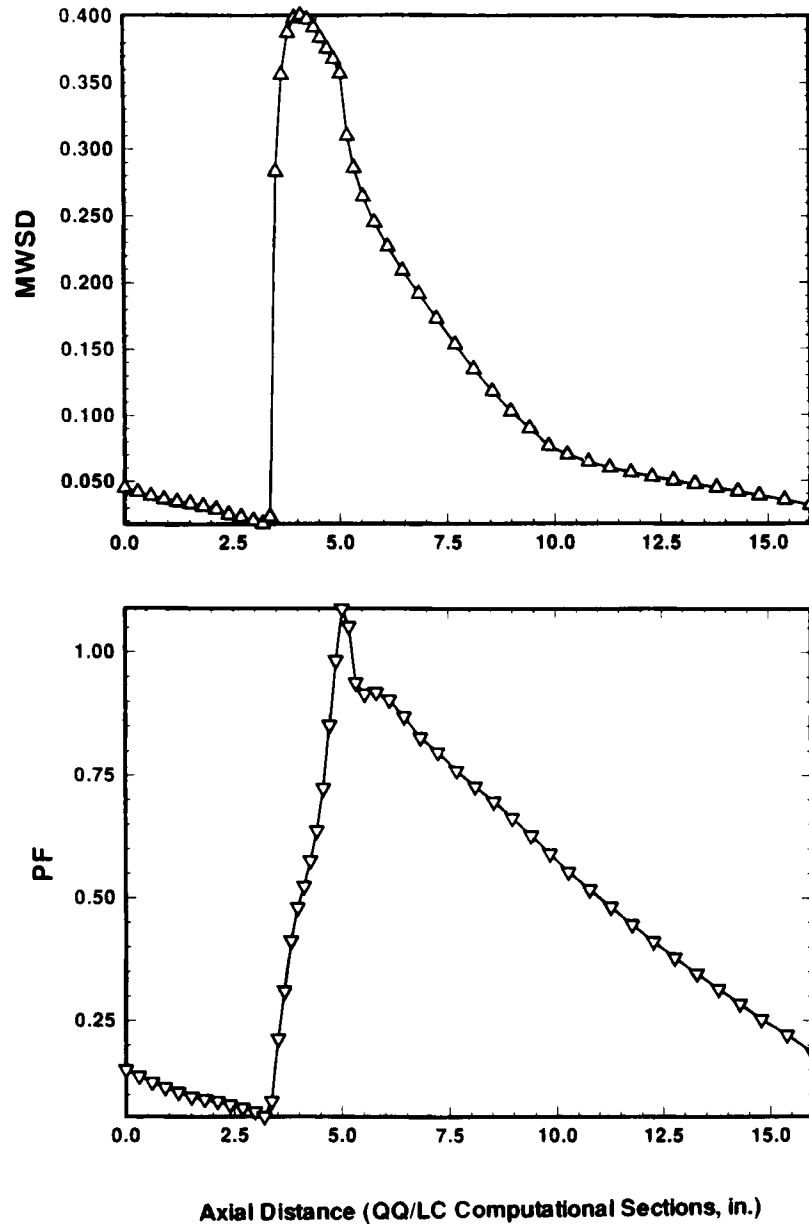

Figure 14. QQ/LC zones MWSD and PF

inlet conditions both at the jet and at the FN/RB zone were chosen similar to those encountered in advanced combustion systems.

Preliminary results illustrate some of the major features of the flow and temperature fields inside the STC. Velocity, temperature and some critical species information inside the FN/RB zone are given. Formation of the co- and counter-rotating bulk flow and the sandwiched-ring-shaped temperature field inside the QQ/LC zones can be seen clearly and is consistent with the experimental observations. The calculations of the MWSD and the PF of temperature

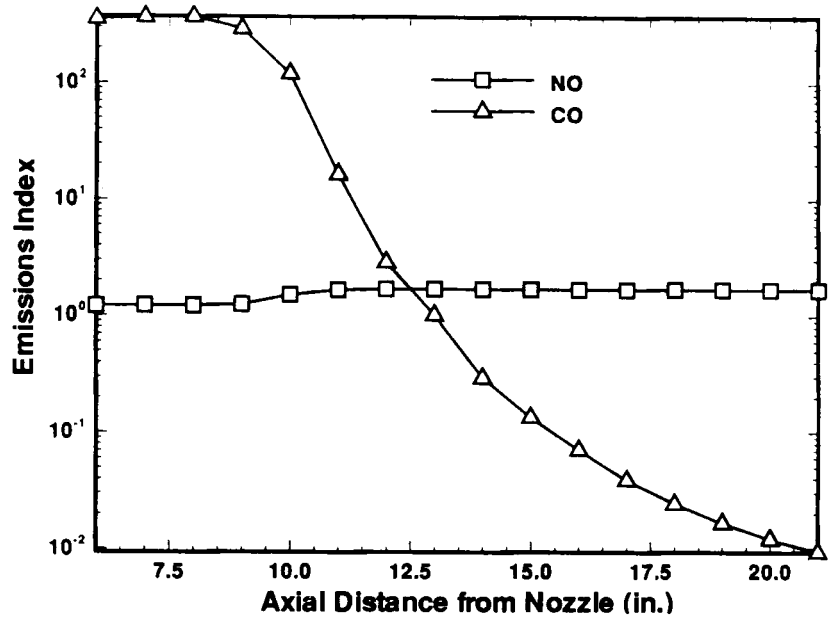

Figure 15. QQ/LC zones CO and NO emission index

revealed that the mixing performance of the STC is very good. The temperature of the fluid leaving the LC zone is very uniform. From the results obtained so far, it appears that the modified KIVA-II code can be used to guide the low-emission combustion experiments.

ACKNOWLEDGEMENTS

The authors thank the NASA Lewis Research Center for funding this work under NASA Contracts NAG3-1109, C-30050-R, and NAG3-1113. Our thanks are also extended to Dr. P. Lee of Fuel Systems Textron for giving us the valuable information regarding the airblast fuel nozzle, Professor S.-J. Ying of the University of South Florida for providing us the kinetic model, and T. D. Butler, A. A. Amsden and P. J. O'Rourke of the Los Alamos National Laboratory for all their help with the KIVA-II code.

REFERENCES

1. A. S. Novick and D. L. Troth, 'Low NO_x heavy fuel combustor concept program'. *NASA CR-165367*, 1981.
2. H. G. Lew, D. R. Carl, G. Vermes, E. A. DeZubay, J. A. Schwab and D. Prothroe, 'Low NO_x heavy fuel combustor concept program, phase I: combustion technology generation Final Report', *NASA CR-165482*, 1981.
3. R. M. Pierce, C. E. Smith and B. S. Hinton, 'Advanced combustion systems for stationary gas turbine engines', 1990, Vol. 3, EPA contract 68-02-2136.
4. F. S. Kemp, R. A. Sederquist and T. J. Rosfjord, 'Evaluation of synthetic fuel character effects on rich–lean stationary gas turbine combustion systems', Vols, 1 and 2, February 1983, EPRI AP-2822, Project 1898-1, Final Report.
5. M. V. Talpallikar, C. E. Smith and M. C. Lai, 'Rapid mix concepts for low emission combustors in gas turbine engines', *CFD Research Co. Report 4090/1*, August 1990.
6. C. E. Smith, M. V. Talpallikar and J. D. Holdeman, 'A CFD study of jet mixing in reduced flow areas for lower combustor emissions', *AIAA-91-2460*, AIAA/SAE/ASME/ASEE 27th Joint Propulsion Conference, Sacramento, CA, 24–26 June 1991.

7. M. V. Talpallikar, C. E. Smith, M. C. Lai and J. D. Holdeman, 'CFD analysis of jet mixing in low NO_x flametube combustors', *ASME paper 91-GT-217*, 36th ASME International Gas Turbine and Aeroengine Conference, Orlando, FL, 3–6 June 1991.
8. N. S. Winoiwich, S. A. Moeykens and H. L. Nguyen, 'Three-dimensional calculation of the mixing of radial jets from slanted slots with a reactive cylindrical crossflow', *AIAA-91-2081*, AIAA/SAE/ASME/ASEE 27th Joint Propulsion Conference, Sacramento, CA, 24–26 June 1991.
9. G. W. Howe, Z. Li, T. I.-P. Shih and H. L. Nguyen, 'Simulation of mixing in the quick quench region of a rich burn–quick quench mix–lean burn combustor', *AIAA-91-0410*, 29th Aerospace Sciences Meeting, Reno, Nevada, 7–10 Jan., 1991.
10. A. A. Amsden, P. J. O'Rourke and T. D. Butler, 'KIVA-II: a computer program for chemically reactive flows with sprays', *Los Alamos National Laboratory Report LA-11560-MS*, May 1989 Los Alamos, NM.
11. D. G. Schweikert, 'An interpolation curve using a spline in tension', *J. Math. Phys.*, **45**, 312–317 (1966).
12. A. K. Cline, 'Scalar- and planar-valued curve fitting using splines under tension', *Commun. ACM*, **17**, 218–220 (1974).
13. C. W. Hirt, A. A. Amsden and J. L. Cook, 'An arbitrary Lagrangian–Eulerian computing method for all flow speeds', *J. Comput. Phys.*, **14**, 227–253 (1974).
14. W. E. Pracht, 'Calculating three-dimensional fluid flows at all speeds with an Eulerian–Lagrangian computing mesh', *J. Comput. Phys.*, **17**, 132–159 (1975).
15. S. L. Yang, M. C. Cline, R. Chen and Y.-L. Chang, 'A three-dimensional algebraic grid generation for gas turbine combustors with inclined slots', ASME International Computers in Engineering Conference and Database Symposium, San Francisco, August 2–6, 1992. Vol. 2, pp. 43–51.
16. W. J. Gordon and C. A. Hall, 'Construction of curvilinear co-ordinate systems and applications to mesh generation', *Int. j. numer. methods eng.*, **7**, 461–477 (1973).
17. R. Haber and J. F. Abel, 'Discrete transfinite mappings for the description and meshing of three-dimensional surfaces using interactive computer graphics', *Int. j. numer. methods eng.*, **18**, 41–66 (1982).
18. H. L. Nguyen and S.-J. Ying, 'Critical evaluation of jet-A spray combustion using propane chemical kinetics in gas turbine combustion simulated by KIVA-II', *AIAA-90-2439*, AIAA/SAE/ASME/ASEE 26th Joint Propulsion Conference, Orlando, FL, 16–18 July, 1990.
19. K. Meintjes and A. P. Morgan, 'Element variables and the solution of complex chemical equilibrium problems', General Motors Research Publication GMR-5827, 1987.